CHAPTER VI

CALCULATIONS AND RESULTS

Using the results from the DACCT measurement, the parameters of the two models, the pseudo-Richardson model in the section 4.1 and the basic model in the subsection 4.3.2, were calculated in this chapter. From the parameters of the pseudo-Richardson model, the effective contact resistance R_c(prm) is calculated in the section6.1. It is compared with the total resistance R_t in Table5 to assert the validity of pseudo-Richardson model. The fitting procedure of the basic model in the subsection 4.3.2 is described in the subsection 6.2.1. From the fitting parameters, at small current where the I-V characteristic is linear, a contact can be quantify by the contact resistivity, the effective contact resistance R_c(fit) is calculated in subsection 6.2.2. Since R_c(fit) is the only resistance of the barrier. Multiplied by the contact area, the result is the lower bound value of the contact resistivity.

6.1 Richardson Plot and Effective Contact Resistance R_c(prm)

From split temperature of each current in Fig.7 and 8, according to eq.4.1.1, B_{eff} and $A_{eff}A^*$ are obtained from the slope and the ordinate intercept, respectively, from the Richardson plot as shown in Fig.14. A_{eff} A^* and B_{eff} of the other contacts are shown in column 2 and 3 of Table 5.

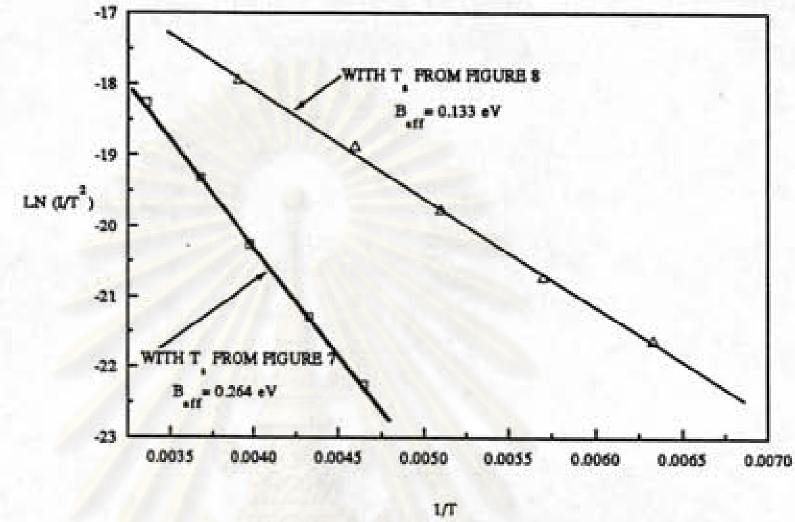

Fig.14 Richardson plot of the data Figs. 7 and 8, yielding the effective barrier height values. The ordinate intercepts yield $A_{eff}\ A^*$ used in calculated R_c(prm).

The straight line obtained from the activation energy plot ,such as in Fig.14, may not be sufficient to justify the validity of the model. [In practice, many experimental data may be fit with a straight line, especially for small data range. For given data there may be more than one model which the plots give straight lines. One should not rely much on justifying the validity of a model having experimental data plottable as a straight line.] The other evidence to assert the validity of the pseudo-Richardson model can be seen as follow.

The theoretical contact resistivity $\rho_c(\text{TE})$, when there is only thermionic emission mechanism for current conduction across the barrier, can be obtained from equation 2.5.2 ,i.e.

$$\rho_c(\text{TE}) = \{k/(qA^*T)\}\ \exp(q\ \phi_{bp}\ /kT) \qquad \Omega\text{ - cm}^2 \qquad (2.5.2)$$

Since pseudo-Richardson model assumed thermionic emission with a barrier height B_{eff}. So the contact resistivity should be calculated as

$$\rho_c = \{k/(qA^*T)\}\ \exp\ (q\ B_{eff}\ /kT) \qquad \Omega\text{ - cm}^2 \qquad (6.1.1)$$

Thus the effective contact resistance R_c(prm), due to the pseudo-Richardson model should be calculated from

$$R_c(\text{prm}) = \{\ k\ /(q\ A_{eff}\ A^*\ T\ )\}\ \exp\ (q\ B_{eff}\ /kT) \quad \Omega \qquad (6.1.2)$$

where $A_{eff}\ A^*$ is obtained from the ordinate intercept in Fig.14. The effective contact resistance values R_c(prm), at 300 K , are shown in Table 5.

TABLE 5

B_{eff}, A_{eff}, and R_c(prm) at room temperature of Au/p-$CuInSe_2$ and Ni/p-$CuInSe_2$

#contact	A_{eff} A* (A/K^2)	B_{eff} (eV)	R_c(prm) (Ω)	R_t (Ω)
B3/5	8.6×10^{-4}	0.318	68	93.0
B6/3/1	1.6×10^{-3}	0.298	17	19.2
C3/20	3.3×10^{-4}	0.264	22*	16.2
D3/4	8.1×10^{-4}	0.274	13	18.9
B6/4	1.9×10^{-3}	0.250	2	6.6
D3/5/2	8.3×10^{-4}	0.280	16	24.3
C3/19	3.4×10^{-4}	0.267	24	29.6
D3/5/1	8.0×10^{-4}	0.231	3	11.2
B4/9/2	1.2×10^{-2}	0.294	2	4.2
C3/16/1	2.0×10^{-3}	0.266	4	9.3
C3/16/2	6.3×10^{-4}	0.227	3	8.9
B6/3/2	1.8×10^{-5}	0.206	44*	23.6
B4/9/1	2.9×10^{-3}	0.272	4	6.3
B4/12/1	4.8×10^{-4}	0.200	1	2.4
B4/12/2	4.3×10^{-5}	0.161	3	3.6
B4/11/5	1.3×10^{-6}	0.111	16*	11.0
B4/11/3	3.2×10^{-6}	0.058	1	1.1
B4/11/1	4.3×10^{-6}	0.111	5	5.2
B4/11/4	2.1×10^{-5}	0.116	1	1.8
B4/11/2	7.1×10^{-6}	0.108	3*	2.7
C3/15/2	9.1×10^{-5}	0.191	5	11.8
C3/15/1	6.3×10^{-5}	0.194	8	13.6
B6/1/2	1.3×10^{-4}	0.181	2	9.1
D3/1	8.1×10^{-5}	0.170	3	10.7
B4/17/2	1.5×10^{-5}	0.16	10*	5.3
B6/1/	4.8×10^{-5}	0.163	3	7.4
D3/3	1.1×10^{-5}	0.156	11	13.3
C3/25/1	1.7×10^{-5}	0.157	7	13.2
C3/25/2	7.6×10^{-6}	0.135	7*	4.0
B4/17/1	8.5×10^{-6}	0.133	6	13.2

where * indicates the case of R_c(prm) greater than R_t. It is obviously impossible in reality, the error should due to a large uncertainty of A_{eff} A^*.

Although the split temperatures is subject to the judgment of the investigator, it does not much effect value of R_c(prm), since a slight decrease of B_{eff} could resulted in large reduction of A_{eff} A^*. For example, it can not justify deliberate correcting the split temperature of #C3/20 to obtain R_c(prm) lower than 20 Ω.

6.2 Fitting Process and Effective Contact Resistance R_c(fit)

6.2.1 Fitting Process

From subsection 4.3, for a given set of parameters, the theoretical value I(V,T) can be calculated according to equation 4.3.2.1 - 4.3.2.8. The parameters included are A_{app}, m^*, m^+, K, ϕ, Δ, N_a(b), N_a(s), and α. Among the nine parameters, m^* ,K are expected to be constant from sample to sample. Here, we chose $m^* = 0.73$ (Neumann, 1986), and K = 13.6 (Wasim, 1986), so there remain 7 parameters to be considered.

For N experimental points I_i , i = 1, 2 , ... N , if one chooses to define the experimental Y_i as (I_i / I_N) , i = 1, 2, ...N - 1, the area dependence is avoided. The corresponding theoretical quantity is $y_{t,i} = J_{t,i} / J_{t,N}$, where the current density is defined in eq. 4.3.2.1, then yields at best fit the values of the remaining six parameters by computer program in Appendix C. The value of $J_{t,i}$ at best fit are then used in the following manner to find A_{app}.

$$A_{app} = \quad [\, I_i / J_{t,i} \,] \qquad (6.2.1.1)$$

Note that a small barrier is the barrier where tunneling is prominent, the latter is sensitive to the barrier shape. Since in this fitting process, the barrier shape is drawn first before calculating the current, so that at the minimum fitting error, the barrier shape should be the correct barrier shape. Thus, this fitting is pertinent for the small barrier.

6.2.1.1 The Result From Au/p-$CuInSe_2$

Table6 shows the data, from the case of the small area metal contact under reverse bias V, the temperature T and the current I. The voltage V is the split voltage, the difference between the two voltage branches in the DACCT measurement of Fig.7, obtained from the range that the lower branch is due to the "bulk".

Also shown in Table6 are the fitting parameters and B_{max}, the zero bias barrier top including image force lowering.

The split voltage should be useable in our model while the lower branch is still smooth, ie. unlike the S-shape of the TFE and neglect TE patterns in figure 18 which shows the blocking of the contact under reverse bias. The smooth of the lower branch ensures that the large area metal still nonblocking. However, for #C3/20, for the current 4.95 mA, using the split voltages at the temperature above 230 K, where the lower branch is still smooth, the recalculated points are nearly the same as in figure 5f. So, in Table 6, we used the split voltages of this current downto 107.1 K, even it is the S-shape.

TABLE 6

Fitting for #C3/20 (Au/p-$CuInSe_2$)

The substrate has resistivity 0.59 Ω-cm, carrier concentration 4.0×10^{17} cm^{-3}.

Contact area 9.5×10^{-3} cm^2

	Input to computer			Output to computer		fitting parameters
i	V (volts)	T (K)	I (A)	$J_{t,i}$ (A / cm^2)	A_i (cm^2)	
1	0.283	107.1	0.00001	0.003739	0.002674	ϕ = 0.5217 eV
2	0.255	137.5	0.00001	0.004923	0.002031	Δ = -0.1761 eV
3	0.174	164.0	0.00001	0.004242	0.002358	$m^+ = 0.07838$
4	0.070	188.0	0.00001	0.004586	0.002181	$N_a(b)=5.32 \times 10^{17} cm^{-3}$
5	0.363	107.1	0.00003	0.011352	0.002643	$N_a(s)=2.15 \times 10^{19} cm^{-3}$
6	0.341	137.5	0.00003	0.015236	0.001969	α = 0.1520 / °A
7	0.267	164.0	0.00003	0.013509	0.002221	$A_{app}=2.32 \times 10^{-3}$ cm^2
8	0.148	188.0	0.00003	0.010665	0.002813	B_{max}=0.455 eV
9	0.486	107.1	0.00010	0.047729	0.002095	
10	0.456	137.5	0.00010	0.055429	0.001804	
11	0.393	164.0	0.00010	0.053311	0.001876	
12	0.283	188.0	0.00010	0.041209	0.002426	
13	0.144	210.6	0.00010	0.037312	0.002680	
14	0.591	107.1	0.00030	0.133614	0.002245	
15	0.567	137.5	0.00030	0.159900	0.001876	
16	0.519	164.0	0.00030	0.172308	0.001741	
17	0.285	210.6	0.00030	0.113979	0.002632	

	Input to computer			Output to computer	
i	V	T	I	$J_{t,i}$	A_i
	(volts)	(K)	(A)	(A / cm^2)	(cm^2)
16	0.519	164.0	0.00030	0.172308	0.001741
17	0.285	210.6	0.00030	0.113979	0.002632
18	0.138	232.2	0.00030	0.123640	0.002426
19	0.720	107.1	0.00103	0.393376	0.002618
20	0.705	137.5	0.00103	0.490522	0.002099
21	0.657	164.0	0.00103	0.516582	0.001994
22	0.577	188.0	0.00103	0.480060	0.002146
23	0.472	210.6	0.00103	0.444245	0.002318
24	0.316	232.2	0.00103	0.379609	0.002713
25	0.162	252.9	0.00103	0.441724	0.002332
26	0.948	107.1	0.00495	1.849683	0.002676
27	0.896	137.5	0.00495	1.771285	0.002795
28	0.833	164.0	0.00495	1.678896	0.002948
29	0.770	188.0	0.00495	1.713124	0.002889
30	0.704	210.6	0.00495	1.903916	0.002599
31	0.624	232.2	0.00495	2.220551	0.002229
32	0.484	252.9	0.00495	2.222402	0.002227
33	0.322	273.0	0.00495	2.441625	0.002027
34	0.155	292.6	0.00495	3.071099	0.001611
35	0.422	188.0	0.00030	0.143272	0.002093

The results of the other Au /p-$CuInSe_2$ are shown in Table 7.

TABLE 7

Fitting parameters for Au /p-$CuInSe_2$

#contact	ϕ (eV)	Δ (eV)	m^+	$N_a(b)$ $x10^{17}$ (cm^{-3})	$N_a(s)$ $x10^{19}$ (cm^{-3})	α $(^oA^{-1})$	A_{app} (cm^2)	B_{max} (eV)
B3/5	0.5680	-0.4415	0.0966	2.44	28.74	0.1460	$4.95x10^{-5}$	0.413
B6/3/1	0.5274	-0.1413	0.0853	4.27	11.12	0.1545	$1.33x10^{-3}$	0.431
C3/20	0.5217	-0.1761	0.07838	5.32	2.15	0.1520	$2.32x10^{-3}$	0.455
D3/4	0.5080	-0.4004	0.0994	4.45	7.67	0.1469	$9.78x10^{-4}$	0.418
B6/3/2	0.5060	-0.2686	0.1258	3.87	26.94	0.1529	$2.20x10^{-5}$	0.360
D3/5/2	0.5017	-0.1266	0.1096	3.73	24.25	0.1529	$8.32x10^{-5}$	0.364
C3/16/2	0.5003	-0.0379	0.0968	5.45	23.53	0.1455	$1.61x10^{-4}$	0.360
C3/16/1	0.4987	-0.1867	0.0908	5.11	4.30	0.1467	$4.67x10^{-3}$	0.424
D3/5/1	0.4848	-0.2355	0.1075	4.42	15.02	0.1454	$6.99x10^{-4}$	0.370
B4/9/2	0.4832	-1.0900	0.0952	1.80	0.83	0.1584	$7.72x10^{-3}$	0.426
B4/9/1	0.4822	-1.3211	0.0565	1.09	0.65	0.1476	$3.07x10^{-3}$	0.430
B6/4	0.4780	-0.1833	0.1076	5.24	13.63	0.1477	$6.40x10^{-4}$	0.368
C3/19	0.4685	-1.2340	0.1168	2.56	12.10	0.1450	$8.03x10^{-6}$	0.360
B4/12/2	0.4652	-0.0411	0.0698	7.16	12.30	0.1442	$1.77x10^{-4}$	0.359
B4/12/1	0.4536	-0.0807	0.0853	5.60	13.13	0.1458	$6.10x10^{-4}$	0.346
B4/11/4	0.4041	-0.4750	0.1010	3.09	13.52	0.1423	$1.11x10^{-4}$	0.294
B4/11/1	0.3976	-0.1898	0.1698	3.24	27.90	0.1437	$3.48x10^{-6}$	0.245
B4/11/3	0.3882	-0.1362	0.1540	7.99	33.73	0.1439	$9.23x10^{-7}$	0.218
B4/11/5	0.3833	-0.3777	0.1234	2.73	18.56	0.1393	$2.28x10^{-6}$	0.256
B4/11/2	0.3608	-0.1833	0.1384	3.05	22.56	0.1436	$3.09x10^{-6}$	0.225

The recalculated of #C3/20 from fitting parameters in Table 6, are shown in Fig. 15.

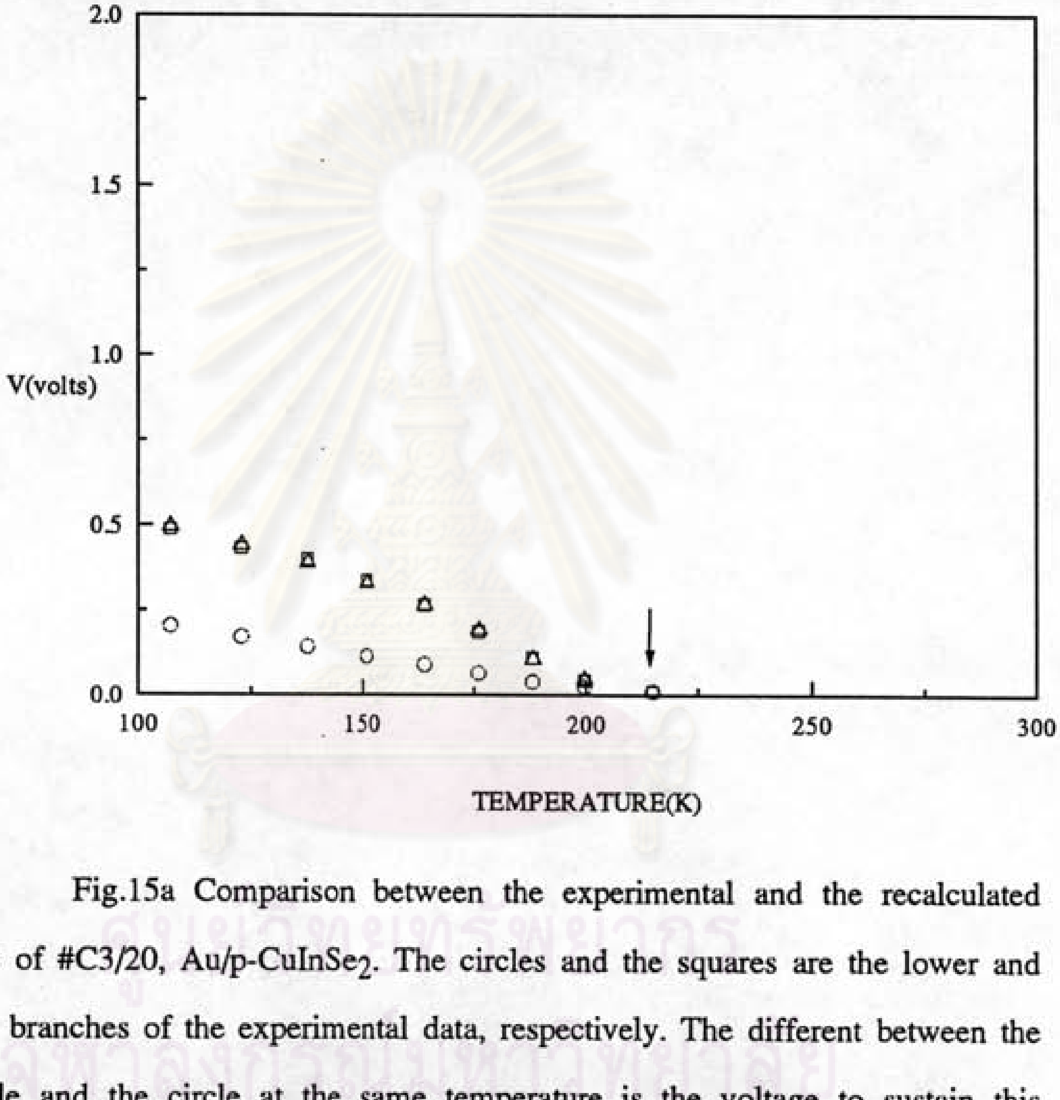

Fig.15a Comparison between the experimental and the recalculated points of #C3/20, Au/p-$CuInSe_2$. The circles and the squares are the lower and upper branches of the experimental data, respectively. The different between the triangle and the circle at the same temperature is the voltage to sustain this constant current which calculated from fitting parameters in Table6. The arrow is the split temperature T_S. In this figure, the current is 0.01 mA.

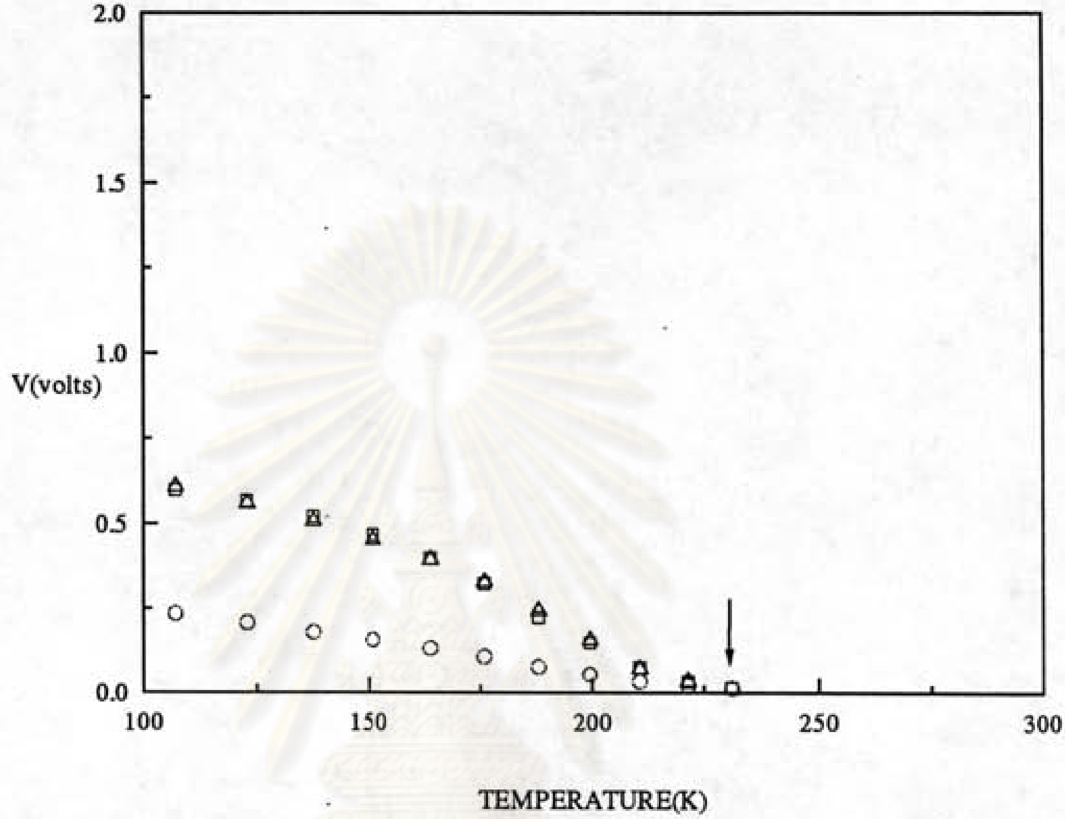

Fig.15b Recalculated and experimental data points of #C3/20 for constant current 0.03 mA.

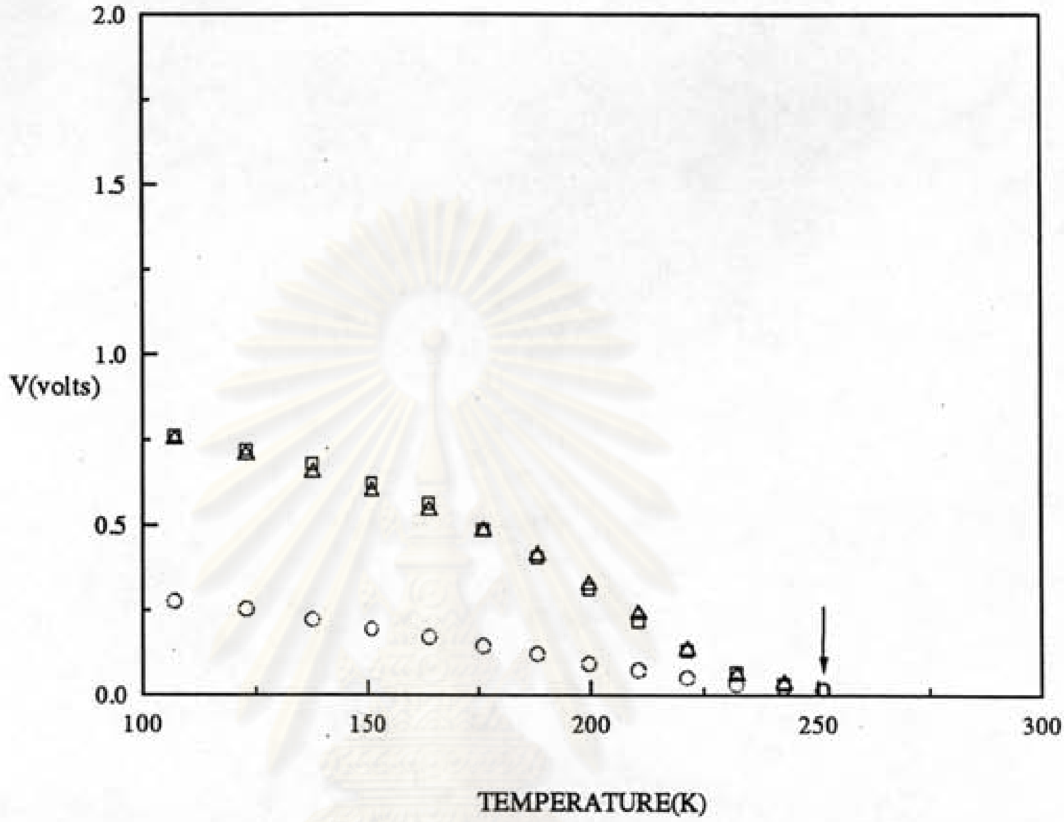

Fig.15c Recalculated and experimental data points of #C3/20 for constant current 0.1 mA.

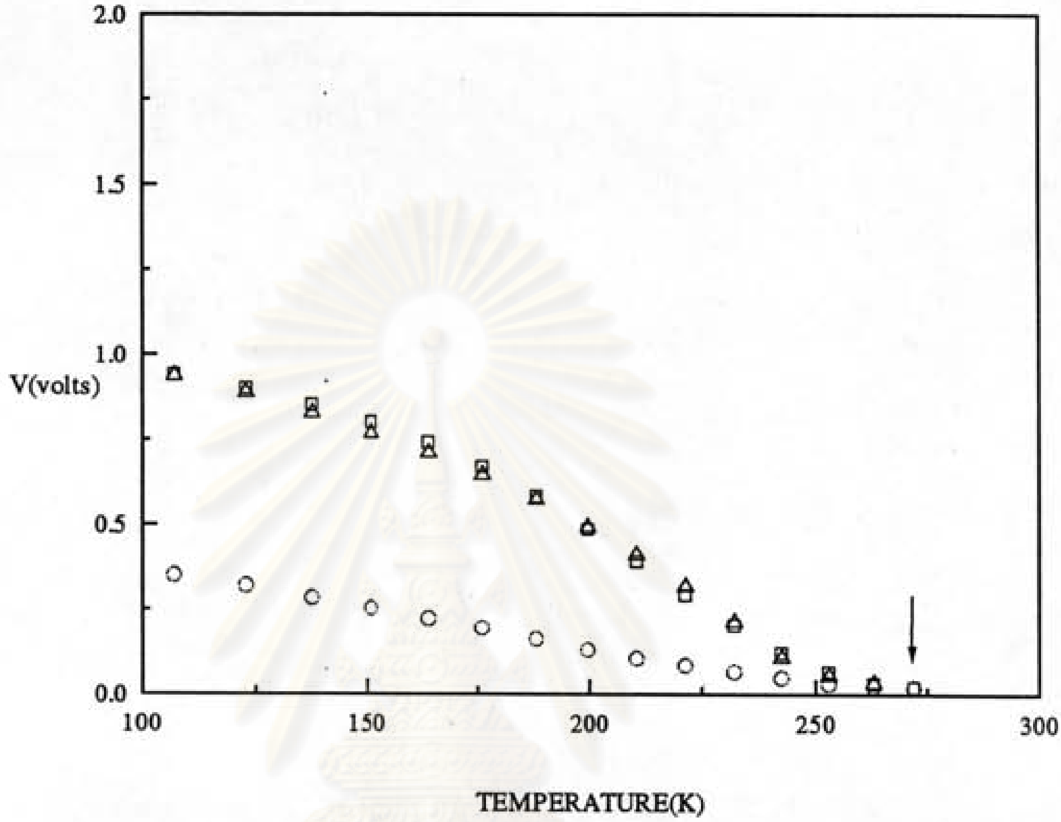

Fig.15d Recalculated and experimental data points of #C3/20 for constant current 0.3 mA

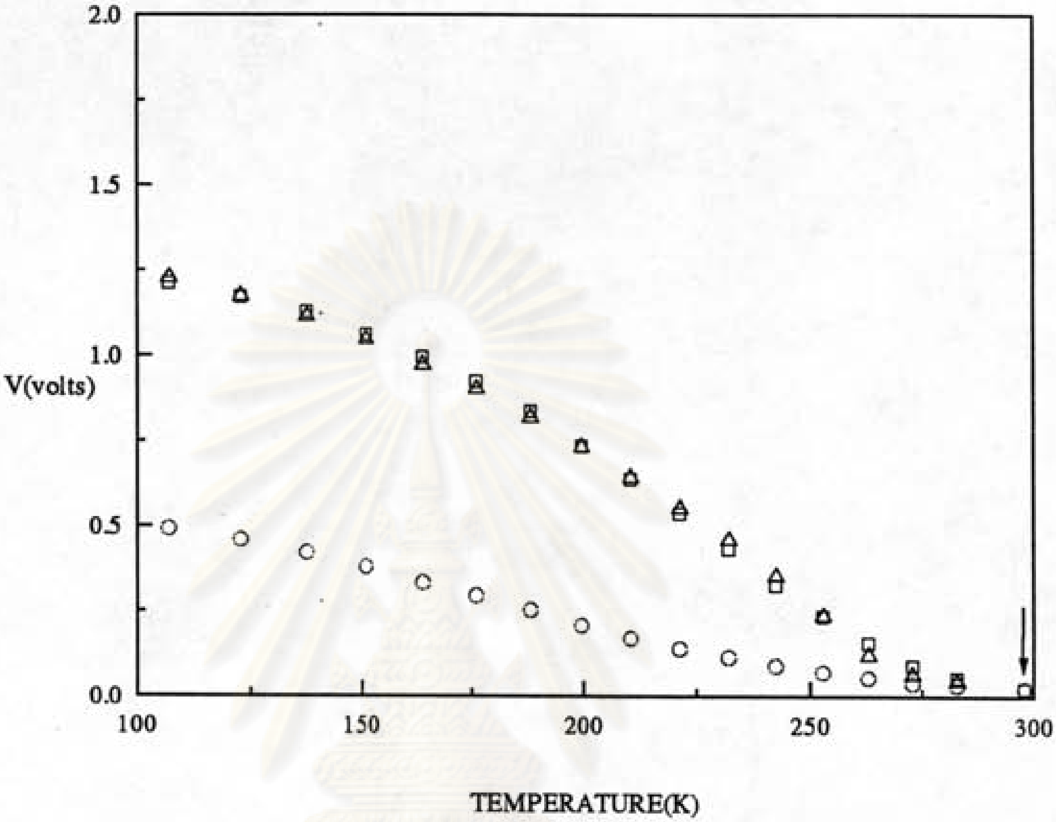

Fig.15e Recalculated and experimental data points of #C3/20 for constant current 1.03 mA.

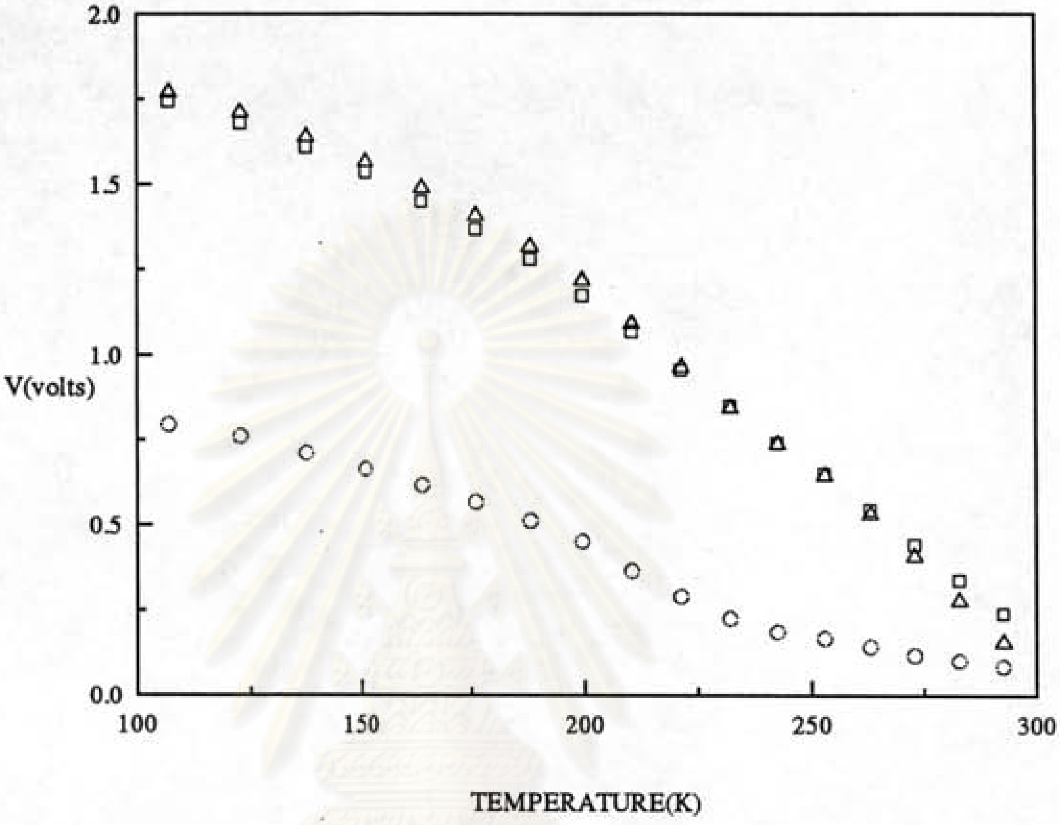

Fig.15f Recalculated and experimental data points of #C3/20 for constant current 4.95 mA.

6.2.1.2 The Result From Ni/p-$CuInSe_2$

Table8 shows the data, from Fig. 8, and the fitting parameters of #C3/25/2.

TABLE 8

Fitting for #C3/25/2 (Ni/p-$CuInSe_2$)

The substrate has resistivity 0.38 Ω - cm, carrier concentration $4.5\times10^{17}cm^{-3}$.

Contact area 9.5×10^{-3} cm^2 .

	Input to computer			Output to computer		fitting parameters
i	V (Volt)	T (K)	I (A)	$J_{t,i}$ ($A\text{-}cm^{-2}$)	A_i (cm^2)	
1	0.053	107.1	0.00001	0.014295	0.0006996	ϕ = 0.2040 eV
2	0.039	123.0	0.00001	0.013679	0.0007311	Δ = - 0.1320 eV
3	0.087	107.1	0.00003	0.031666	0.0009474	m^+ = 0.08331
4	0.079	123.0	0.00003	0.035467	0.0008459	$N_a(b)=11.42\times10^{17}cm^{-3}$
5	0.058	137.5	0.00003	0.031138	0.0009635	$N_a(s)=-38.77\times10^{19}$ cm^{-3}
6	0.137	107.1	0.00010	0.086481	0.0011563	α = 0.1236 $^oA^{-1}$
7	0.137	123.0	0.00010	0.109893	0.0009099	$A_{app}=1.17\times10^{-3}$ cm^2
8	0.121	137.5	0.00010	0.107432	0.0009308	B_{max}=0.412 eV
9	0.100	151.0	0.00010	0.100171	0.0009983	
10	0.054	164.0	0.00010	0.061567	0.0016242	
11	0.187	107.1	0.00030	0.207814	0.0014444	
12	0.196	123.0	0.00030	0.294757	0.0010177	

	Input to computer			Output to computer	
i	V	T	I	$J_{t,i}$	A_i
	(Volt)	(K)	(A)	($A\text{-}cm^{-2}$)	(cm^2)
11	0.187	107.1	0.00030	0.207814	0.0014444
12	0.196	123.0	0.00030	0.294757	0.0010177
13	0.190	137.5	0.00030	0.334981	0.0008956
14	0.144	164.0	0.00030	0.283192	0.0010593
15	0.102	176.0	0.00030	0.206771	0.0014509
16	0.045	188.0	0.00030	0.122311	0.0024528
17	0.258	107.1	0.00103	0.604916	0.0017027
18	0.272	123.0	0.00103	0.869020	0.0011852
19	0.275	137.5	0.00103	1.083356	0.0009507
20	0.274	151.0	0.00103	1.298560	0.0007931
21	0.260	164.0	0.00103	1.357276	0.0007588
22	0.233	176.0	0.00103	1.234640	0.0008342
23	0.185	188.0	0.00103	0.909709	0.0011322
24	0.129	199.5	0.00103	0.634213	0.0016241
25	0.067	210.6	0.00103	0.432335	0.0023824
26	0.341	107.1	0.00495	1.737786	0.0028484
27	0.360	123.0	0.00495	2.497273	0.0019821
28	0.376	137.5	0.00495	3.449762	0.0014348
29	0.386	151.0	0.00495	4.471162	0.0011071
30	0.395	176.0	0.00495	6.842834	0.0007233
31	0.390	188.0	0.00495	7.892477	0.0006272
32	0.369	199.5	0.00495	8.009955	0.0006179

i	Input to computer V (Volt)	T (K)	I (A)	Output to computer $J_{t,i}$ (A-cm-^{2})	A_i (cm^2)
31	0.390	188.0	0.00495	7.892477	0.0006272
32	0.369	199.5	0.00495	8.009955	0.0006179
33	0.334	210.6	0.00495	7.344326	0.0006739
34	0.283	221.5	0.00495	6.045607	0.0008188
35	0.220	232.2	0.00495	4.666984	0.0010606
36	0.154	242.6	0.00495	3.712153	0.0013334
37	0.111	252.9	0.00495	3.815691	0.0012972
38	0.076	263.0	0.00495	4.259461	0.0011621
39	0.394	164.0	0.00495	5.716886	0.0008658
40	0.178	151.0	0.00030	0.356157	0.0008423

The recalculated of #C3/25/2 from fitting parameters in Table 8, is shown in Fig.16. Note that at high current and low temperature, the recalculating significantly deviate from the experimental, unlike Fig.15. All Ni/p-$CuInSe_2$ contacts show this effect. So, the basic model in section 4.3.2 does not fit with Ni/p-$CuInSe_2$ contact.

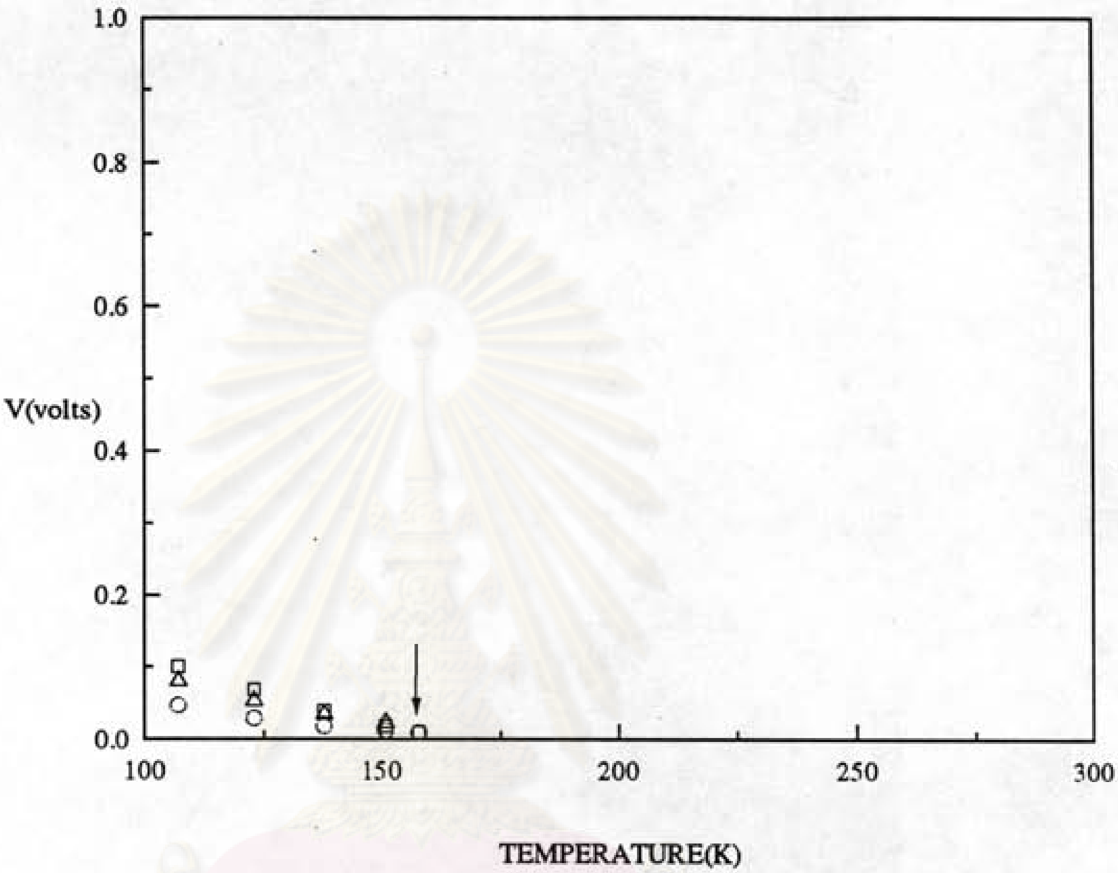

Fig.16a Comparison between the experimental and the recalculated points of #C3/25/2, Ni/p-$CuInSe_2$. The circles and the squares are the lower and upper branches of the experimental data, respectively. The different between the triangle and the circle at the same temperature is the voltage to sustain this constant current which calculated from fitting parameters in Table8. The arrow is the split temperature T_S. In this figure, the current is 0.01 mA.

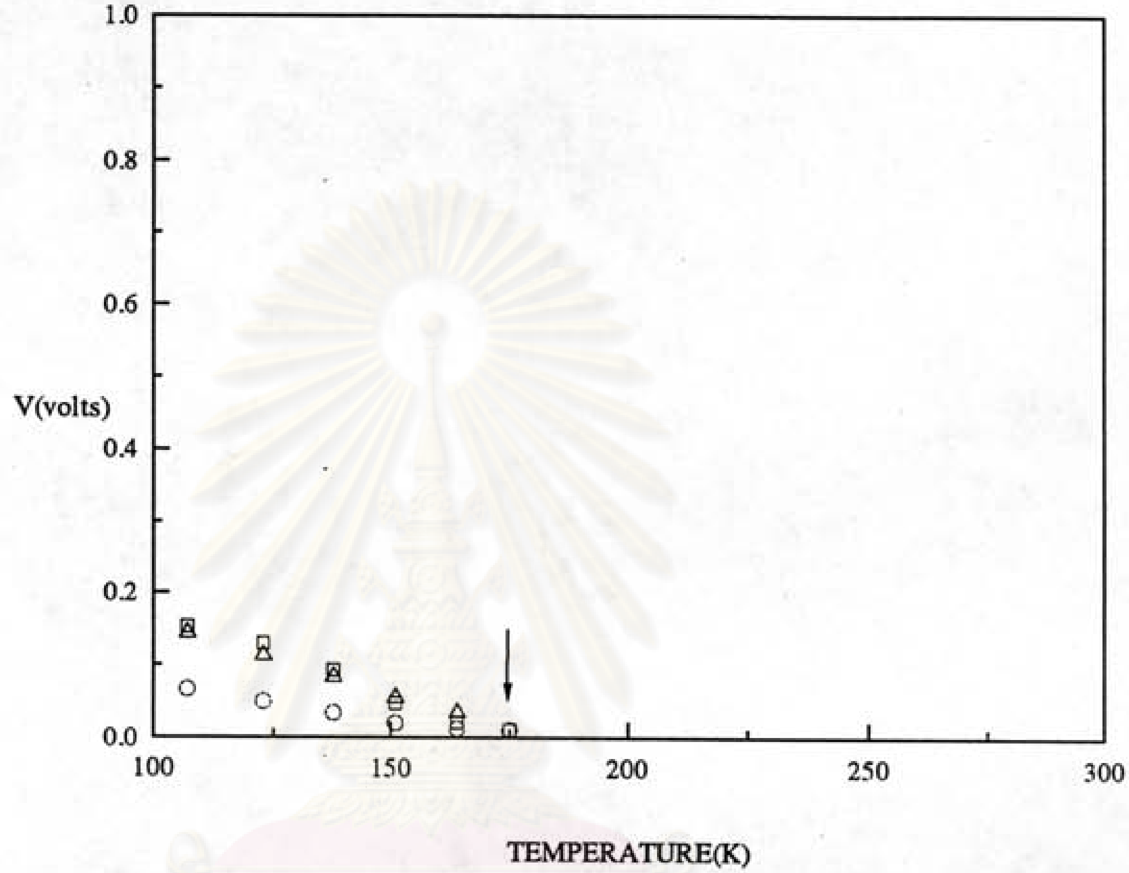

Fig.16b Recalculated and experimental data points of #C3/25/2 for constant current 0.03 mA.

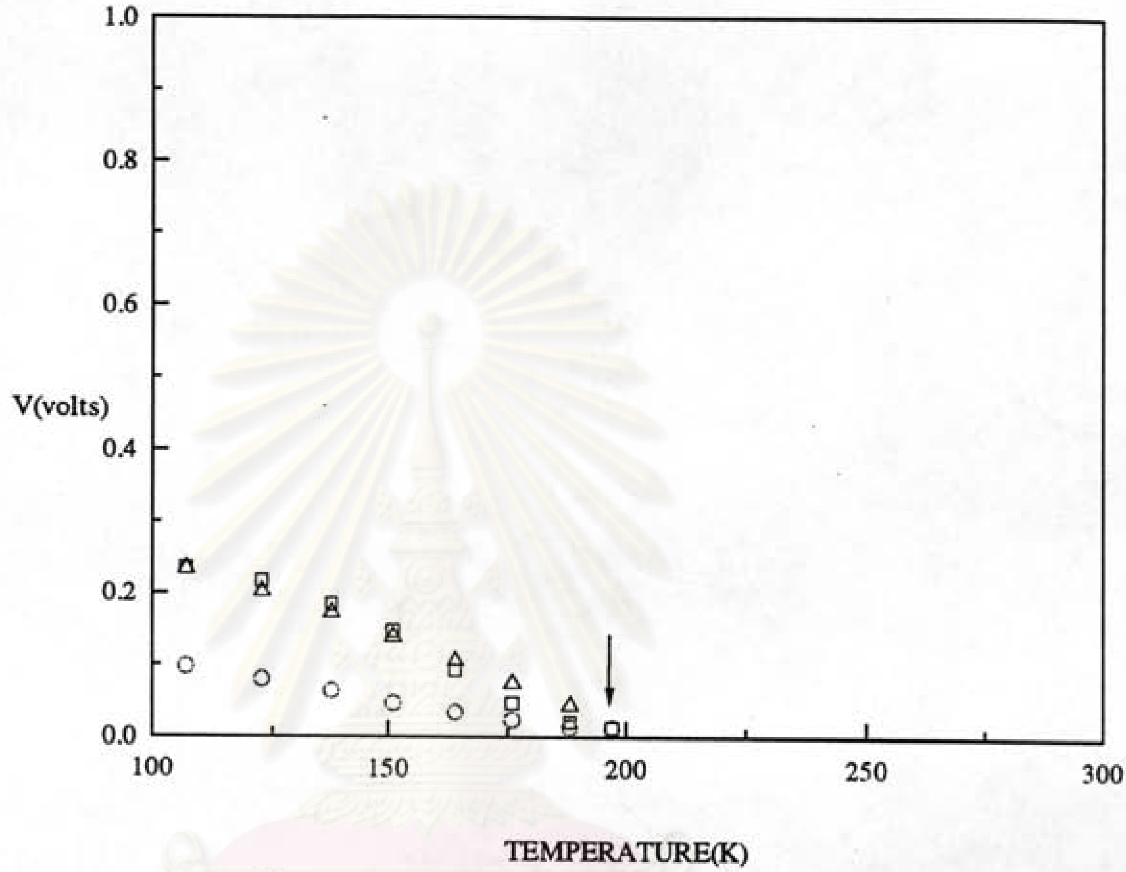

Fig.16c Recalculated and experimental data points of #C3/25/2 for constant current 0.1 mA.

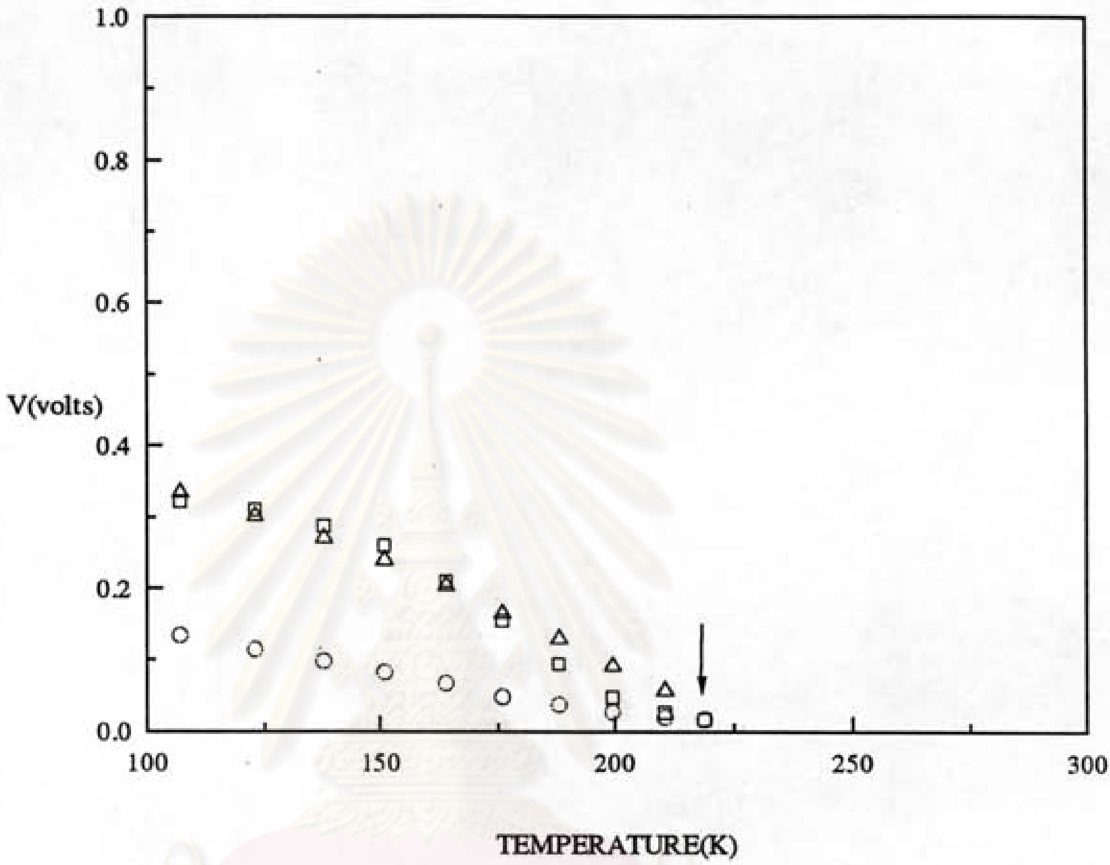

Fig.16d Recalculated and experimental data points of #C3/25/2 for constant current 0.3 mA.

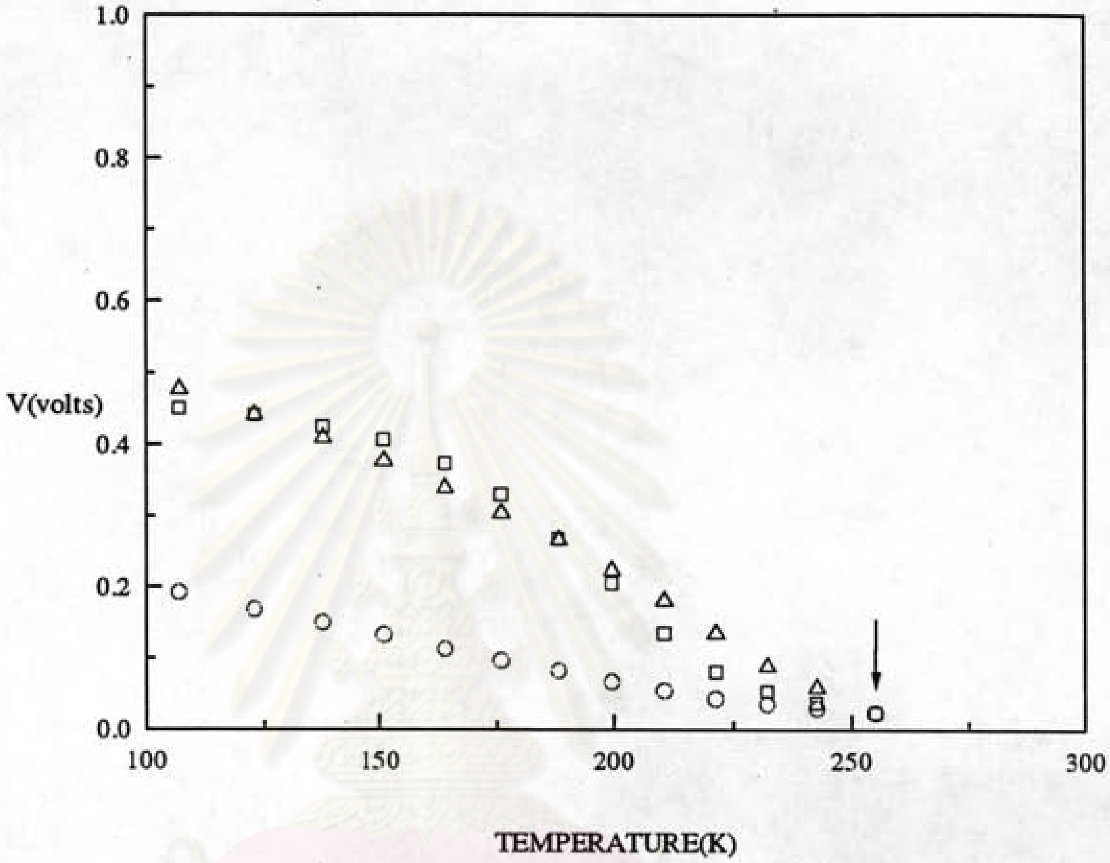

Fig.16e Recalculated and experimental data points of #C3/25/2 for constant current 1.03 mA.

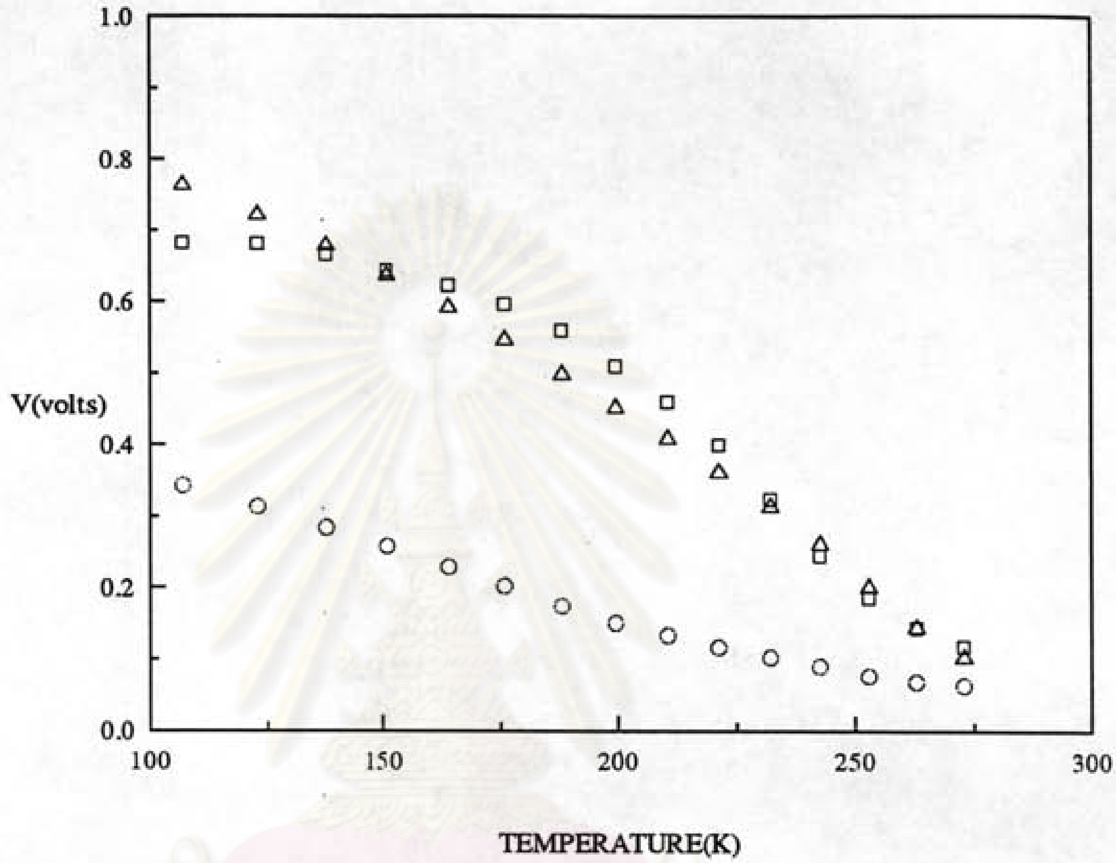

Fig.16f Recalculated and experimental data points of #C3/25/2 for constant current 4.95 mA.

6.2.2 Effective Contact Resistance R_c(fit)

Assumed that for a small forward current there still no other mechanisms involve, except the thermionic-field emission as in the reverse, the forward current should be governed by the same barrier's parameters. From the fitting (barrier's) parameters in subsection 6.2.1, i.e. ϕ, Δ, m^+, $N_a(b)$, $N_a(s)$, α and A_{app}, both forward and reverse current at small bias are calculated. For reverse current, the equation 4.3.2.1- 4.3.2.8 are directly used. But for the forward current, the bias voltage in section 4.3 is -V. So, the boundary at x = S, in eq.4.3.2.6 become :

$$B(S; -V) = + V + \Delta \qquad (6.2.2.1)$$

and V in eq. 4.3.2.7 and 4.3.2.8 change sign for the case of the forward bias. The calculation of the currents at bias voltages -4, -3, -2, -1, 0, 1, 2, 3 and 4 mV, at 300 K, from fitting parameters in Table6 are shown in Fig.17. The bias voltages are chosen in the sense that the current density (current per the contact area) govern the maximum current density of p-$CuInSe_2$ solar cells (40 mA/cm^2). The effective contact resistance R_c(fit) was calculated from the slope. It was the resistance of the contact in the range which independent to bias, the contact can be quantify by the contact resistivity.

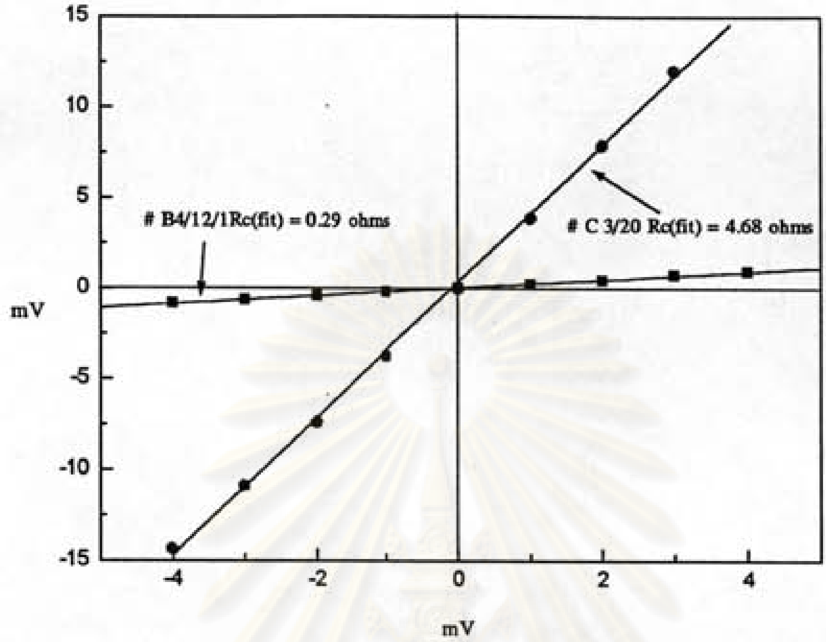

Fig.17 I-V characteristics at 300 K and small current of #C3/20 and #B4/12/1, Au/p-$CuInSe_2$. The fitting parameters used in the calculation are from Table 7.

R_c(fit) of the other contacts, calculated in the same manner of #C3/20 and #B4/12/1 above, of Au/p-$CuInSe_2$ are shown in Table9. Total resistance R_t and contact area (from Table2) are also shown. The former for comparison with R_c(fit). The latter for lower bound contact resistivity ρ_c(min) calculation. This can be accomplished by multiply R_c(fit) with the contact area.

TABLE 9

Effective contact resistance R_c(fit) at 300 K that calculated from fitting parameters in Table7.

#sample	contact area (cm^2)	R_c(fit) (Ω)	R_t (Ω)	ρ_c(min) (Ω-cm^2)
B3/5	$9.5x10^{-3}$	14.48	93.0	0.148
B6/3/1	$9.5x10^{-3}$	4.10	19.2	0.039
C3/20	$9.5x10^{-3}$	4.68	16.7	0.045
D3/4	$9.5x10^{-3}$	2.60	18.9	0.025
B6/3/2	9.5x10-3	8.42	23.6	0.080
D3/5/2	9.5x10-3	3.94	15.2	0.037
C3/16/2	$9.5x10^{-3}$	1.05	8.9	0.010
C3/16/1	9.5x10-3	0.93	9.3	0.009
D3/5/1	9.5x10-3	0.61	5.6	0.006
B4/9/2	9.5x10-3	0.87	6.6	0.008
C3/19	9.5x10-3	25.27	29.6	0.240
B4/12/2	9.5x10-3	0.95	2.7	0.009
B4/12/1	9.5x10-3	0.29	2.4	0.003
B4/11/4	$5.7x10^{-2}$	0.22	1.8	0.013
B4/11/1	$4.4x10^{-3}$	0.95	5.2	0.004
B4/11/3	$2.8x10^{-2}$	0.39	1.1	0.011
B4/11/5	$4.4x10^{-3}$	2.70	11.0	0.011
B4/11/2	$9.5x10^{-3}$	0.72	2.7	0.007